Computation of the Self-Similarity Region of a Turbulent Round Jet Using Large-Eddy Simulation

Christophe Bogey[1] and Christophe Bailly[2]

[1] Laboratoire de Mécanique des Fluides et d'Acoustique
Ecole Centrale de Lyon, UMR CNRS 5509
69134 Ecully, France
christophe.bogey@ec-lyon.fr
[2] Same address
christophe.bailly@ec-lyon.fr

Summary. A round free jet at Reynolds number $\mathrm{Re}_D = 11000$ is computed by Large Eddy Simulation on a grid of 44 million nodes containing a part of the self-similarity region of the flow. Turbulence properties in this region, including second- and third-order moments of velocity, pressure-velocity correlations and kinetic energy budget, are calculated. They are compared to, and complement, the experimental results of Panchapakesan & Lumley [1] for a jet at the same Reynolds number.

1 Introduction

The turbulent round jet is a model flow that has been extensively investigated experimentally since fifty years. Two flow regions have been displayed: the initial-development region and, farther downstream, the self-preservation region where the flow profiles are self-similar. Turbulence in the first region was studied in some detail in the sixties by Sami [2]. Turbulence in the self-similar region was also characterized by Wygnanski & Fiedler [3] for a jet at Reynolds number $\mathrm{Re}_D = 10^5$ ($\mathrm{Re}_D = u_j D/\nu$ where u_j and D are the jet nozzle-exit velocity and diameter, and ν the molecular viscosity). In the zone where self-preservation was observed, some 70 diameters downstream of the nozzle, Wygnanski & Fiedler [3] measured many flow quantities including mean velocity, turbulence stresses and triple correlations, and calculated the kinetic energy balance across the jet. Despite some uncertainties in the measurements and the different processes involved in the evaluation of the energy terms, their results were fairly accurate. They were reference solutions, until the early nineties and the experimental data obtained by Panchapakesan & Lumley [1] and Hussein *et al.* [4] in the self-similarity regions of jets at respectively $\mathrm{Re}_D = 1.1 \times 10^4$ and $\mathrm{Re}_D = 10^5$.

Panchapakesan & Lumley [1] and Hussein *et al.* [4] (hereafter referred to as P&L and HC&G) reported careful measurements of the second- and third-order moments of velocity, and used them to evaluate the energy balance across the jet self-similarity region. However some turbulence quantities, such as the pressure-velocity correlations or the moment $<v'w'^2>$ (v' and w' are the fluctuating radial and azimuthal velocities and $< . >$ is the statistical average), could not be measured, and the energy dissipation could not be directly calculated. Therefore P&L neglected the pressure diffusion in the energy budget and obtained the dissipation profile as the closing balance, whereas HC&G estimated energy dissipation from measurements assuming isotropy or axisymmetry of small scales, and obtained the pressure diffusion as the remaining term.

Considering these experimental weaknesses, numerical simulations may appear as one appropriate way to describe exhaustively the turbulence developing in jets, because they give access to all flow quantities. The limitations in this case are due to the computational resources, and might originate from the numerical methods and the turbulence models involved in the simulations. Direct Numerical Simulation (DNS) can be used for flows at low Reynolds numbers, as shown by Mansour *et al.* [5] for a turbulent channel flow. However, for flows at higher Reynolds numbers, typically those investigated experimentally, one must make use of Large Eddy Simulation (LES), where only the turbulent scales larger than the grid size are calculated. Dejoan & Leschziner [6] for example recently computed in this way the energy budget in a plane turbulent wall jet at a moderate Reynolds number.

In the present work, a circular jet at Mach number $\mathrm{M} = u_j/c_0 = 0.9$ (c_0 is the sound speed in the ambient medium) and at Reynolds number $\mathrm{Re}_D = 1.1 \times 10^4$ is simulated by LES. This Reynolds number corresponds exactly to the Reynolds number of the experimental jet of P&L. The LES is performed using numerical schemes with low dissipation and low dispersion [7], and is based on the use of selective filtering as subgrid modelling [8, 9, 10]. The computational domain includes 44 million nodes, and is sufficiently large to contain a part of the jet self-similarity region. The aim is to investigate the turbulence properties in this region by calculating, directly from the LES data, turbulence quantities such as the second- and third-order moments of velocity fluctuations, the pressure-velocity correlations, and all the terms in the kinetic energy budget. The present results are systematically compared to the P&L data, when those are available. This will allow us to assess the LES accuracy, and to discuss the assumptions made by P&L, as well as by HC&G, for evaluating the energy terms across the jets. Reliable informations on jet turbulence physics are also expected to be obtained.

2 Simulation parameters

An isothermal round jet at Mach and Reynolds numbers $\mathrm{M} = u_j/c_0 = 0.9$ and $\mathrm{Re}_D = 1.1 \times 10^4$ is simulated. The LES is performed on a Cartesian grid using numerical schemes with spectral-like properties [7], optimized in the wavenumber space to be low-dissipative and low-dispersive for waves discretized by more than four grid points. The spatial discretization is taken into account by explicit finite-differences and selective filtering, using both eleven-point stencils. The time advancement is carried out using a six-stage low-storage Runge-Kutta algorithm. The selective filtering is applied explicitly every second iteration to remove the grid-to-grid oscillations without affecting the resolved scales, but also to provide the effects of the subgrid energy-dissipating scales. The LES approach based on explicit filtering has been successfully used by different authors for various flows [8, 11, 12, 13]. It has been shown in particular that the filtering does not artificially decrease the effective flow Reynolds number unlike subgrid models based on eddy-viscosity [9]. The effects of the filtering have been also investigated from the energy budget [10].

The computational domain is discretized by a Cartesian grid of $651 \times 261 \times 261$ nodes, and extends up to 182 radii in the axial direction and to 33 radii in the transverse directions. As in our previous simulations [8], the boundary conditions are non-reflective. A sponge zone is used at the outflow, restricting the physical part of the domain to 150 radii downstream. This is illustrated by the vorticity snapshot of Figure 1, where the development of the flow in axial direction is also clearly visible. As for the jet initial conditions, mean velocity profiles are imposed at the jet inflow, while random velocity disturbances are added to seed the turbulence. The axial mesh spacing is $\Delta x = r_0/4$, and the transverse mesh spacing is $\Delta y = \Delta y_0 = r_0/8$ near the centreline, but $\Delta y = r_0/4$ for $y \geq 7r_0$. The time step is $\Delta t = 0.85\Delta y_0/c_0$.

In the present study, all the terms in the energy budget are calculated explicitly from the LES data as in [14]. For their statistical convergence, the simulation time is necessarily important. The results presented in this paper are obtained from a simulation of 350000 time steps, leading to a physical time of $Tu_j/D = 16700$. The statistics are computed during the final 270000 time steps, or $Tu_j/D = 12900$. Note finally that the present LES required 22.4 Gb of memory and 2100 CPU hours using a Nec SX5.

3 Results

The development of the jet flow towards self-similarity is investigated in figure 2 where centreline profiles of mean and turbulence quantities are represented. In the self-preserving jet, the centreline mean velocity u_c and the jet half-width $\delta_{0.5}$ are indeed respectively given by $u_c/u_j = B \times D/(x - x_0)$ and $\delta_{0.5} = A \times (x - x_0)$, where B and A are two constants, and x_0 denotes a

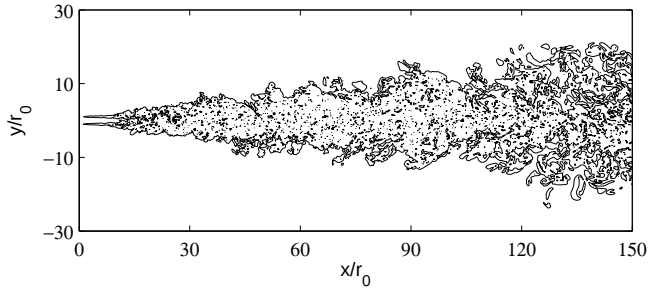

Fig. 1. Snapshot of the vorticity field in the plane $z = 0$. Representation of the two contours associated with the magnitudes of the vorticity norm $|\boldsymbol{\omega}| \times x/u_j = [4, 40]$.

virtual origin. The self-similarity of the turbulent flow is also reached when the turbulence intensities display constant values on the jet axis.

The variation along the jet axis of the mean axial velocity is shown in figure 2(a). For $x \geq 50r_0$, the centreline velocity appears to decrease following the x^{-1} law, with a decay constant of $B = 6.4$. A fair agreement with the results of P&L is also observed, which, however, reflect a slightly lower decay constant of $B = 6.06$. For brevity, the evolution of the jet half-width is not presented here, but note that it is found to increase linearly for $x \geq 50r_0$, at the spreading rate $A = 0.086$. For comparison, P&L obtained $A = 0.096$.

The axial variations of turbulence intensities are shown in figure 2(b). Both the axial and the radial components appear to increase up to about $x = 100r_0$, where self-similar values of $u'_{rms}/u_c = 0.24$ and $v'_{rms}/u_c = 0.2$ seem to be reached. These evolutions along the jet axis compare well with the data of P&L, which are also plotted in the figure and exhibit self-similar values of $u'_{rms}/u_c = 0.24$ and $v'_{rms}/u_c = 0.19$.

The present profiles support that, for the simulated jet, the self-similarity of the mean flow is observed for $x \geq 50r_0$, but that the similarity of the turbulent flow is found farther downstream, for $x \geq 100r_0$. This trend agrees with experimental results of Wygnanski & Fiedler [3] or of P&L.

The profiles across the jet of the mean axial and radial velocities normalized with u_c, obtained over the range $70r_0 \leq x \leq 130r_0$, are shown in figures 3(a) and (b). The LES mean axial velocity agrees very well with the self-similarity profile measured by P&L. A good similarity is also seen for the mean radial velocity profile predicted by the LES and the profile obtained by P&L from the mean axial velocity using the continuity equation. The negative values of the mean radial velocity for large distances from the axis indicate the entrainment of the surrounding fluid into the jet flow.

The radial profiles of turbulence intensities, computed over the range $100r_0 \leq x \leq 140r_0$, are presented in figure 4. Both their shapes and their magnitudes compare well with the results of P&L in the self-preserving jet. The agreement is in particular very good for the axial component u'_{rms} and for the Reynolds stress $<-u'v'>$.

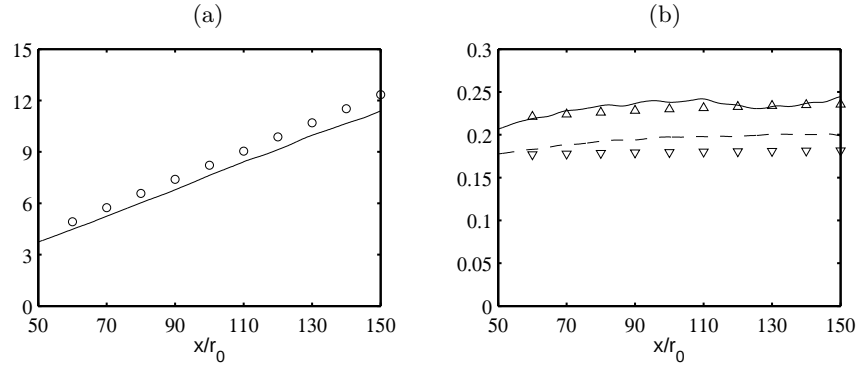

Fig. 2. Variations along the jet centreline. (a) Inverse of mean axial velocity, u_j/u_c: ——— LES, o P&L. (b) Turbulence intensities, u'_{rms}/u_c: ——— LES, △ P&L, and v'_{rms}/u_c: – – – LES, ▽ P&L.

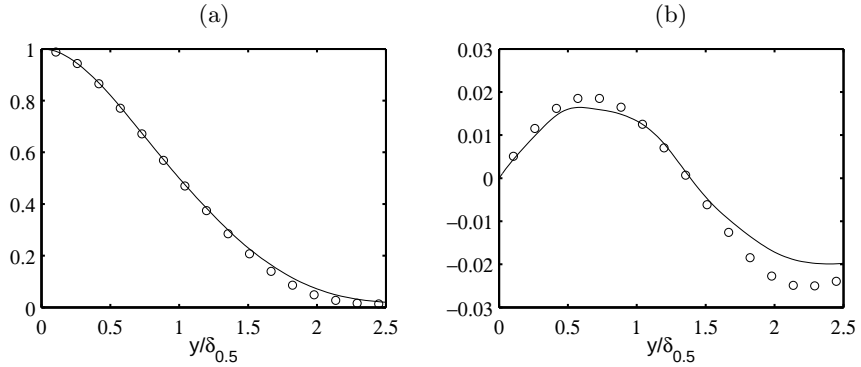

Fig. 3. Mean velocity profiles across the jet, (a) axial velocity, and (b) radial velocity: ——— LES, o P&L. The LES profiles are averaged over $70r_0 \leq x \leq 130r_0$, $\delta_{0.5}$ is the jet half-width.

For the evaluation of the different terms in the energy budget, LES provides all turbulent quantities that are necessary, including those that are often not available from the experiments. Two examples are given in figure 5 with the pressure-velocity correlations and third-order moments of velocity.

The radial profiles of pressure-velocity correlations $<p'u'>$ and $<p'v'>$, computed from the LES data, are shown in figure 5(a). These results are of interest since these correlations cannot be measured experimentally, and are therefore usually evaluated thanks to turbulence models. They are for instance estimated in HC&G from the energy dissipation curves assuming isotropic or axisymmetric turbulence.

The third-order moments of velocity fluctuations $<v'^3>$ and $<v'w'^2>$ computed by LES are presented in figure 5(b). The profile of $<v'^3>$ across the jet is found to be very close to the P&L measurements. The profile of

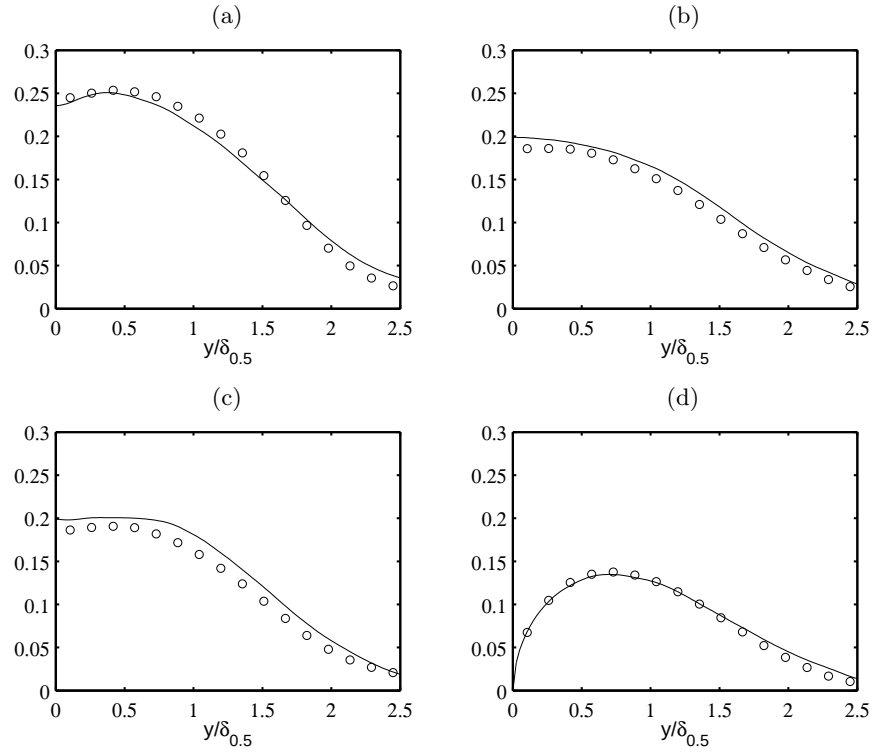

Fig. 4. Turbulence intensities of the velocity fluctuations across the jet, (a) u'_{rms}/u_c, (b) v'_{rms}/u_c, (c) w'_{rms}/u_c, and (d) $<-u'v'>^{1/2}/u_c$: ——— LES, o P&L. The LES profiles are averaged over $100r_0 \leq x \leq 140r_0$.

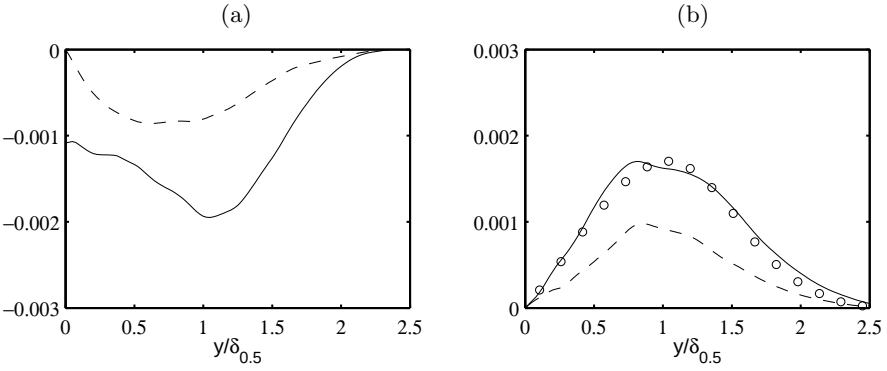

Fig. 5. Variations across the jet. (a) Pressure-velocity correlations obtained by LES: ——— $<p'u'>/(\rho_c u_c^3)$, – – – $<p'v'>/(\rho_c u_c^3)$. (ρ_c and u_c are the mean centerline density and velocity.) (b) Third-order moments of velocity fluctuations, $<v'^3>/u_c^3$: ——— LES, o P&L, $<v'w'^2>/u_c^3$: – – – LES. The LES profiles are averaged over $100r_0 \leq x \leq 140r_0$.

$<v'w'^2>$ shows a similar shape, but has a magnitude which is about half of the magnitude of the previous moment. With this result in mind it may be useful mentioning that the assumption $<v'w'^2>=<v'^3>$ is frequently made in calculations of the turbulent diffusion term in the energy budget using experimental data.

The budget of the turbulent kinetic energy in the jet self-similarity region is now presented. All the terms of the budget, including those derived from the filtered compressible Navier-Stokes equations [10] and those due to the explicit selective filtering [14], are computed directly from the LES fields. The profiles across the jet of the main energy terms are shown in figure 6. These terms correspond to mean flow convection, production, dissipation, turbulent diffusion and pressure diffusion, the dissipation term being here the sum of the viscous dissipation and of the filtering dissipation.

The LES results are compared to the experimental results of P&L for a jet at the same Reynolds number. There is an excellent agreement for the four curves associated with convection, production, dissipation and turbulent diffusion. The pressure-diffusion term calculated by LES, albeit not negligible, is found to be small with respect to the other energy terms. The P&L hypothesis that this term can be neglected in the evaluation of the energy budget then appears relevant. The present results finally cast doubt on the energy budget obtained experimentally by HC&G for a jet at a higher Reynolds number where, using various turbulence modellings, dissipation is found to be about twice as large as in P&L, and pressure diffusion is of the order of mean flow convection.

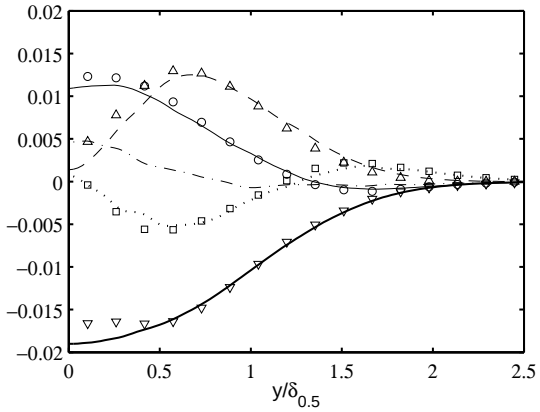

Fig. 6. Kinetic energy budget across the jet: mean flow convection (——— LES, o P&L), production (– – – LES, △ P&L), dissipation (——— LES, ▽ P&L), turbulent diffusion (····· LES, □ P&L), and pressure diffusion (– · – · LES). The curves are normalized by $\rho_c u_c^3 \delta_{0.5}$, and averaged over $100r_0 \leq x \leq 140r_0$.

4 Concluding remarks

The first LES results of a round jet at Reynolds number $\mathrm{Re}_D = 11000$, that is being performed to investigate the self-similarity region of the flow, are presented in this paper. These results, including mean flow and turbulence properties, are shown to compare very well with the measurements of P&L for a jet at the same Reynolds number. The agreement is particularly striking for the turbulent kinetic energy budget, for which P&L used different assumptions. By providing all flow quantities, LES gives us an opportunity to evaluate the turbulent features, such as pressure-velocity correlations, that might not be available experimentally. The computational cost is however quite high, and the present simulation is to be continued to have fully converged triple correlations of velocity and energy terms. Further results will also deal with the component energy budgets.

Acknowledgments

The authors gratefully acknowledge the Institut du Développement et des Ressources en Informatique Scientifique (IDRIS - CNRS) for providing computing time and for its technical assistance.

References

1. Panchapakesan NR, Lumley JL (1993) J. Fluid Mech. 246:197–223
2. Sami S (1967) J. Fluid Mech. 29(1):81–92
3. Wygnanski I, Fiedler H (1969) J. Fluid Mech. 38(3):577–612
4. Hussein HJ, Capp SP, George WK (1994) J. Fluid Mech. 258:31–75
5. Mansour NN, Kim J, Moin P (1988) J. Fluid Mech. 194:15–44
6. Dejoan A, Leschziner MA (2005) Phys. Fluids A, 17(2):025102
7. Bogey C, Bailly C (2004) J. Comput. Phys. 194(1):194–214
8. Bogey C, Bailly C. (2005) Computers and Fluids (available online)
9. Bogey C, Bailly C (2005) AIAA Journal 43(2):437–439
10. Bogey C, Bailly C (2005) In proceedings of Turbulence and Shear Flow Phenomena-4 (2):817–822 To appear in Int. J. Heat Fluid Flow (2006)
11. Stolz S, Adams NA, Kleiser L (2001) Phys. Fluids 2001 13(4):997–1015
12. Mathew J, Lechner R, Foysi H, Sesterhenn J, Friedrich R (2003) Phys. Fluids 15(8):2279–2289
13. Rizzetta DP, Visbal MR, Blaisdell GA (2003) Int. Journal for Numerical Methods in Fluids 42(6):665–693
14. Bogey C, Bailly C (2003) In proceedings of Direct and Large-Eddy Simulation V 23–30